JOURNAL OF MATERIALS SCIENCE 33 (1998) 827–831

Thermal conductivity of $RAlO_3$ (R = Dy, Er and Ho) in liquid helium temperatures

T. NUMAZAWA, H. KIMURA
National Research Institute for Metals, 1-2-1 Sengen, Tsukuba 305, Japan
K. SHIMAMURA, T. FUKUDA
Institute for Materials Research, Tohoku University, Sendai 980-77, Japan

The thermal conductivities of rare earth ortho-aluminate, $DyAlO_3$, $ErAlO_3$ and $HoAlO_3$, single crystals were measured between 2 and 20 K at magnetic fields between 0 and 5 T. In zero magnetic field, the thermal conductivities show a typical dielectric behaviour and there are large differences in the peak values of the thermal conductivities. This suggests that the resonant phonon scattering by rare earth ions already exists at zero magnetic field in those perovskites. Two types of magnetic field dependencies are observed. The thermal conductivities of $DyAlO_3$ and $ErAlO_3$ decrease with increasing magnetic field; however, $HoAlO_3$ gives the opposite result. These dependencies can be qualitatively explained by using an energy level scheme on the ground state in Kramer or non-Kramer ions.

1. Introduction

This paper gives experimental results and qualitative analyses of thermal conductivity in rare earth ortho-aluminates, $DyAlO_3$, $ErAlO_3$ and $HoAlO_3$, at temperatures in the liquid helium range and at magnetic fields varying between 0 and 5 T. Recently, these materials have received attention as magnetic refrigerants for liquid helium production because of the appropriate magnetic transition temperatures and large magnetic moments of rare earth ions [1]. $DyAlO_3$ has been widely studied in terms of its magnetic, optical and thermal properties as an example of complexed antiferromagnetic and metamagnetic ordering [2–6]. For $ErAlO_3$ and $HoAlO_3$, however, there have been few data available for the study of magnetic refrigeration [7]. We have reported the entropy properties based on magnetization measurements [8]. In the present paper, we will describe the heat transport mechanism of these perovskites at low temperatures.

2. Experimental procedure

The rare earth ortho-aluminate, $DyAlO_3$, $ErAlO_3$ and $HoAlO_3$, single crystals were grown with the directions of their c-axes using the Czochralski method. The size of each crystal was 10 mm in diameter and 50 mm in length. Characterization of these single crystals shows that they have the structure of the simple perovskite showing orthorhombic distortion. Some dislocations and iridium inclusions are observed [9], particularly in the crystal of $DyAlO_3$.

The thermal conductivity measurements were made in a helium cryostat in which the sample, in the form of a rod 4 cm in length and 6 mm^2 in cross-section, was mounted within an evacuated container. A NbTi superconducting magnet was set around the sample chamber so that the magnetic field was applied parallel to the length of the sample with the c-axis up to 5 T of the maximum field. The temperature of the helium could be maintained constant at temperatures around 2 K. A heater that was wound on the free end of the sample was used to maintain the temperature gradient along it, with the gradient being measured by two carbon glass thermometers (Lakeshore CGR series). The accuracy of the measurements was estimated to be within $\pm$ 10% error.

3. Results and discussion

3.1. Zero magnetic field conductivity

The thermal conductivities, (λ), of $DyAlO_3$, $ErAlO_3$ and $HoAlO_3$ in a zero magnetic field are shown in Fig. 1 on a logarithmic plot. As a reference, the thermal conductivity of an SiO_2 single crystal, which is a typical high thermal conductor, is also inserted in Fig. 1. The figure shows a decrease in conductivity with decreasing temperature, which is typical of a dielectric crystal at low temperatures. In this case the heat transport is predominantly via phonons. The thermal conductivities of these crystals depend on the perfection of the crystals in the liquid helium temperature. The experimental data show that they are high thermal conductors, in particular λ of $ErAlO_3$ is comparable to that of SiO_2. Although some dislocations and inclusions are found in the sample [9], the results show that the perfection of the samples will be high enough. In such nearly perfect crystals, the low temperature thermal conductivities mainly depend on the boundary scattering, which is determined by the sizes of the samples. In the present experiment the samples

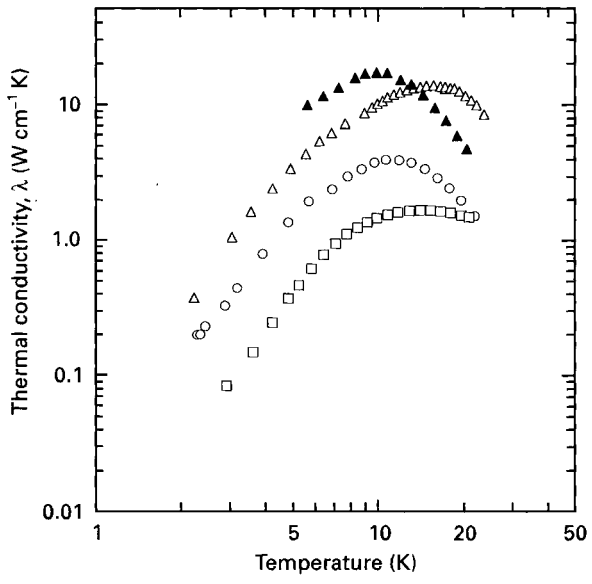

Figure 1 Experimental results on thermal conductivity in zero magnetic field: (○) $DyAlO_3$, (△) $ErAlO_3$ and (□) $HoAlO_3$, (▲) SiO_2 single crystal.

are almost equal in size. Thus, another phonon scattering mechanism should be considered. It is known in some rare earth garnet crystals that resonant phonon scattering by rare-earth ions reduces the thermal conductivity [10]. The dominant scattering process is such that a single phonon is absorbed when a 4f-shell electron of a rare earth ion makes a transition between two different electronic levels of its ground-state manifold. Then, a similar phonon is remitted in a direction uncorrelated with that of the original one. As shown in Fig. 1, λ decreases in the series Er, Dy and Ho, and a similar tendency has been found in the rare earth gallium garnets, such as $Dy_3Ga_5O_{12}$, $Er_3Ga_5O_{12}$ and $Ho_3Ga_5O_{12}$. Comparing the λ of $DyAlO_3$ with our previous experimental result [11] on $Dy_3Ga_5O_{12}$, the $DyAlO_3$ perovskite has a higher thermal conductivity than that of the $Dy_3Ga_5O_{12}$ garnet. In general, the larger the number of optic branches in the phonon spectrum, the lower the thermal conductivity [10]. Garnets have many optic modes due to 80 atoms in the large primitive unit cell, while perovskites have 25 atoms. This implies that the rare earth perovskites may have higher thermal conductivities than garnets because of their simple crystal structures.

3.2. Non-zero magnetic field conductivity

All perovskite samples show strong correlations between the thermal conductivity, λ, and the magnetic field, B. Figs 2a, 3a and 4a show the magnetic field dependence of λ versus temperature, T, curves for $DyAlO_3$, $ErAlO_3$ and $HoAlO_3$, respectively. Figs 2b, 3b and 4b also show the magnetic field dependence, but the data are plotted in the form of λ versus B at a constant temperature of 15 K. The figures at first sight indicate a remarkable difference; two types of magnetic field dependence. The λ of $DyAlO_3$ and $ErAlO_3$ decrease with increasing B and the minimum λ is observed at around 2.5 T in Figs 2b and 3b. On the contrary, $HoAlO_3$ shows the opposite result. The λ

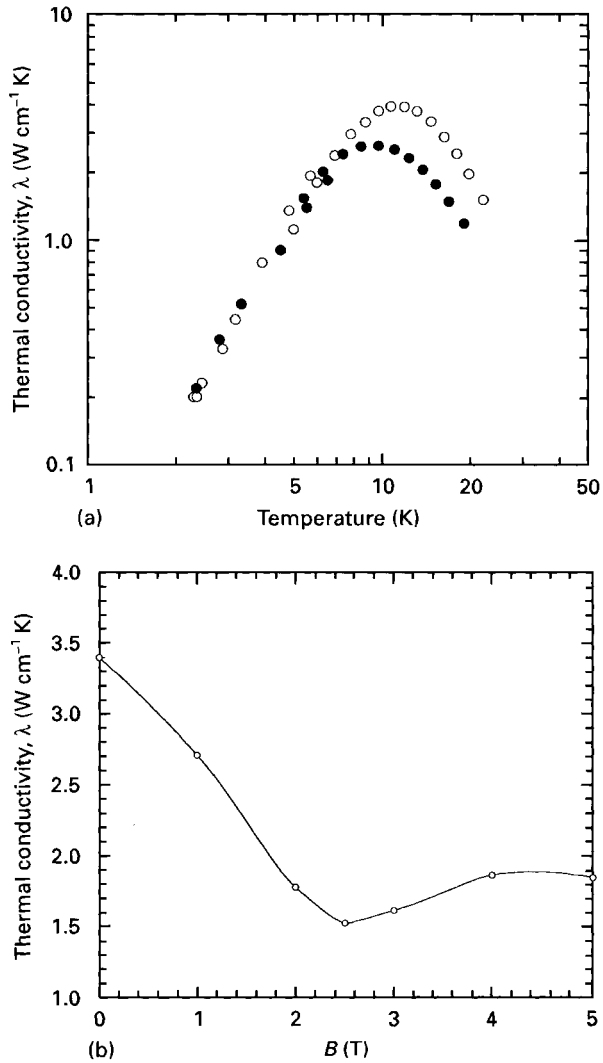

Figure 2 Magnetic field B, dependence of thermal conductivity, λ, in $DyAlO_3$: (a) λ versus T plot, and (b) λ versus B plot at $T = 15$ K. In (a) $B = 0$ T (○), $B = 5$ T (●).

increases as B is increased and approaches a broad peak around 5 T as seen in Fig. 4b.

The magnetic field dependence of thermal conductivity at low temperatures has been found in several paramagnetic salts. The fundamental scheme of the phonon scattering is as follows; the applied magnetic field splits or changes the energy level of the ground state, for example, the ground state doublet will be split by $g\beta B$, where g is the spectroscopic splitting factor and β is the Bohr magneton. If phonons are present at this energy level they will induce transitions between the doublet levels and will therefore be scattered.

More details will be discussed after McClintock *et al.* [12]. The phonon thermal conductivity can be represented by the Debye specific heat theory (Callaway's formula [13]) as

$$\lambda = CT^3 \int_0^{\Theta/T} f(\varkappa)\,[l(\varkappa)\,d\varkappa] \qquad (1)$$

and

$$f(\varkappa) = \frac{\varkappa^4 e^{\varkappa}}{(e^{\varkappa} - 1)^2} \qquad (2)$$

where $\varkappa = g\beta B/\kappa T$ and κ and Θ are the Boltzmann and Debye constants, respectively. C is a constant

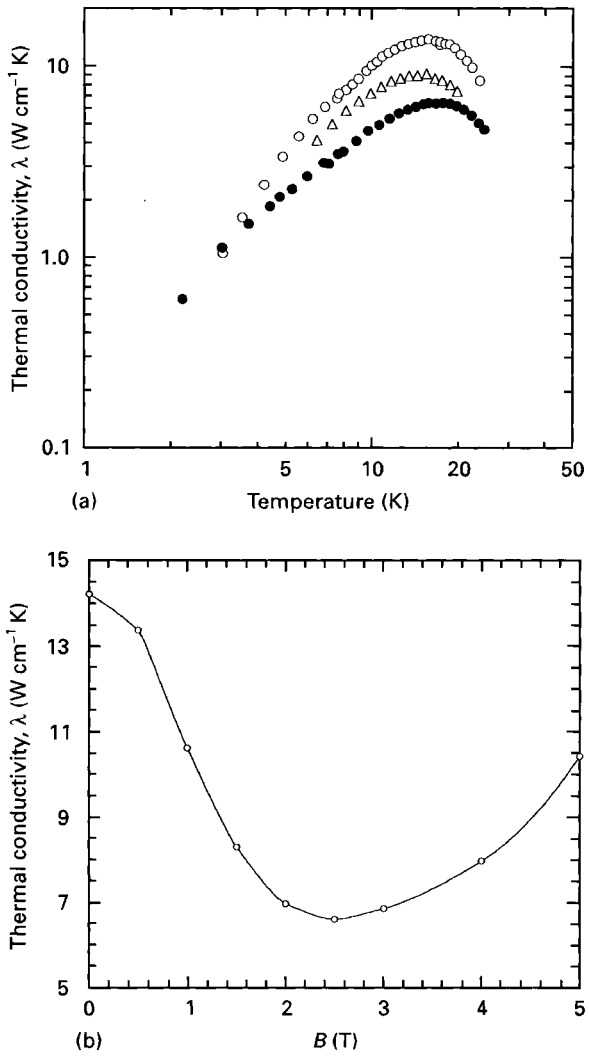

Figure 3 Magnetic field, B, dependence of thermal conductivity, λ, in $ErAlO_3$: (a) λ versus T plot, and (b) λ versus B plot at $T = 15$ K. In (a) $B = 0$ (○), $B = 2.5$ T (●) and $B = 5$ T (△).

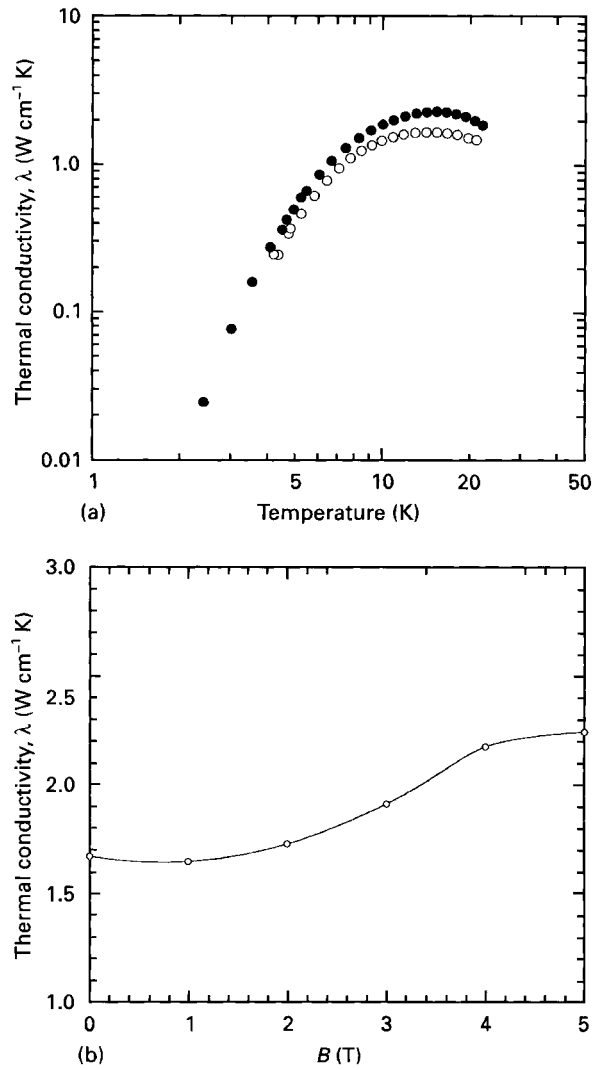

Figure 4 Magnetic field, B, dependence of thermal conductivity, λ, in $HoAlO_3$; (a) λ versus T plot, and (b) λ versus B plot at $T = 15$ K. In (a) $B = 0$ T (○), $B = 5$ T (●).

given by the mean sound velocity of the material. The $l(\varkappa)$ is the mean free path of the phonons that consists of several factors, such as boundaries, impurities, defects, three-phonon processes and resonant type scatterings. Because the perovskite samples are nearly perfect dielectric crystals, only resonant scattering based on the splitting energy will be considered here. In this case, we may assume that $l(\varkappa)$ is constant, i.e. the sample has only boundary scattering except for the resonant one. Fig. 5 shows the form of the integrand in Equation 1 where $l(\varkappa) = 1$, namely, $f(\varkappa)$ given by Equation 2. Clearly, the integral of $f(\varkappa)$ is proportional to the number of phonons that can contribute to the heat transport. At low temperatures, $2 \sim 3$ T of the magnetic field is enough to provide a sufficient splitting energy, $\Delta E \sim \kappa T$. A typical example of $\varkappa = g\beta B/\kappa T = 4$ is shown in Fig. 5 as the shaded area. A certain width of the band of phonons at $\varkappa = 4$ will be removed by the resonant form, and as a result the thermal conductivity decreases.

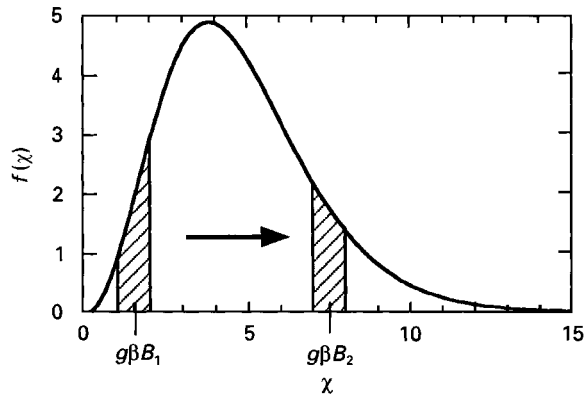

Figure 5 The form of the integrand in Equation (1) in the case of $l(\varkappa) = 1$. The shaded area is proportional to the number of phonon removed by the resonant scattering form on applying a magnetic field at $\varkappa = g\beta B/\kappa T = 4$.

Both $DyAlO_3$ and $ErAlO_3$ perovskites show antiferromagnetic behaviour and the Neel temperatures are estimated to be 3.5 and 0.6 K, respectively. Because Dy and Er are Kramer ions, degeneracy of the Kramer doublet will be present at the ground state. The doublet can only be split by the magnetic field as shown schematically in Fig. 6a. At a fixed temperature, $\varkappa$ is proportional to B and the number of resonant phonons changes with B as $f(\varkappa)$, shown in Fig. 6b. When applied to a magnetic field, λ decreases

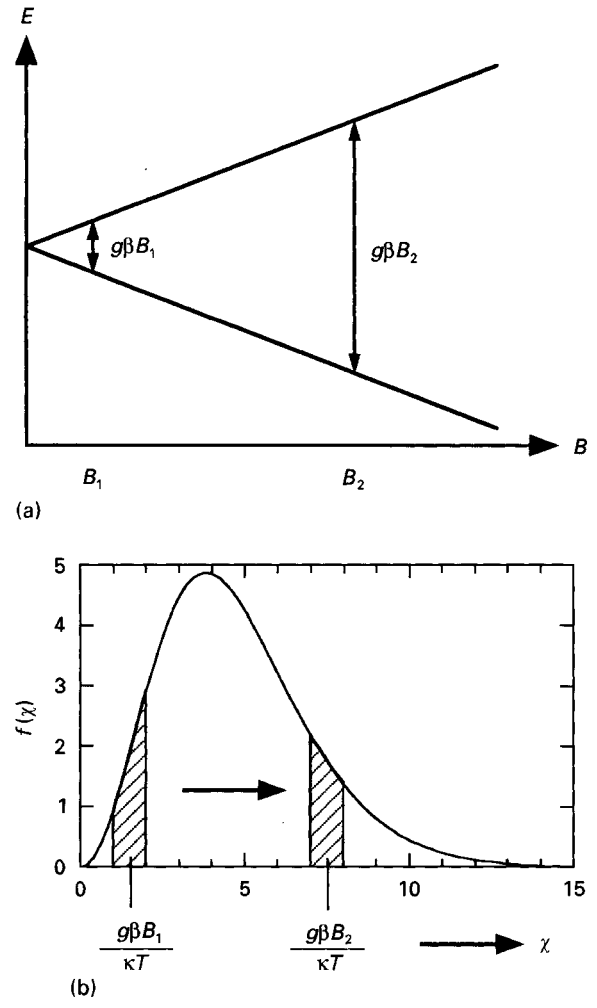

Figure 6 (a) Schematic representation of energy bands in the case of the Kramer doublet; (b) the energy splitting is proportional to the magnetic field, B, and the energy difference is $\Delta E = g\beta B$.

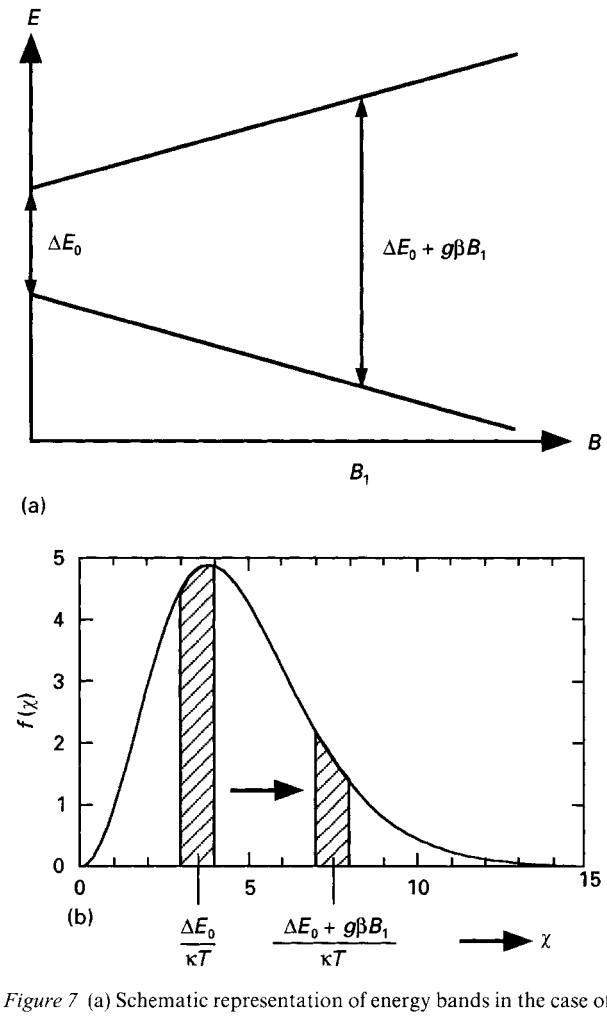

Figure 7 (a) Schematic representation of energy bands in the case of the Kramer doublet split in zero magnetic field; (b) the energy difference is $\Delta E = \Delta E_0 + g\beta B$, where ΔE_0 is a split energy at $B = 0$.

because the number of phonons removed increases, and passes a minimum at a magnetic field, B_m, where the integrand $f(\chi)$ reaches a maximum value, and then increases. Thus, the simple scheme roughly explains the experimental results on the λ versus B curve for $DyAlO_3$ and $ErAlO_3$ in Figs 2b and 3b. In Fig. 2b, λ has a broad peak between 40 and 5 T. This suggests that the higher energy level should also be considered in the case of $DyAlO_3$ because of many low lying energy levels at low temperatures [7].

For $HoAlO_3$, we consider a simple energy scheme of Ho^{3+} because of the few data available on magnetic and optic properties. In general, Ho^{3+} is a non-Kramer ion where the ground state multiplet is 5/8. The ground state doublet will already be split by the crystal field at low temperatures as shown in Fig. 7a. In this case, there is already phonon scattering due to the split energy of ΔE_0 at $B = 0$. As shown in Fig. 7b, $\chi_0 = \Delta E_0/\kappa T$ is slightly smaller than χ_m, which gives the maximum of $f(\chi)$. This is because λ has a broad minimum around 1 T as seen in Fig. 4b and the number of phonons removed at χ_0 should be smaller than that at χ_m. As B increases, the number of phonons removed reaches a maximum at χ_m and then it decreases for $B > 1$ T. Such an unusual magnetic field dependence of thermal conductivity will be one of the typical examples to be found in a non-Kramer ion.

4. Conclusions

The basic mechanism of phonon scattering in those perovskites tested here will be similar to that of the garnet crystals. Mixing rare-earth ions in these materials controls the magnetic field dependence of thermal conductivity. Especially, $ErAlO_3$ has considerably high thermal conductivity and will be useful as a dielectric thermal conductor. An unusual magnetic field dependence in $HoAlO_3$ will be applicable to a unique thermal switch that magnetic field enhances thermal conductivity.

References

1. M. D. KUZ'MIN and A. M. TISHIN, *J. Appl. Phys.* **24** (1991) 2039.
2. L. M. HOLMES, L. G. VAN UITERT, R. R. HECKER and G. W. HULL, *Phys. Rev. B* **5** (1972) 138.
3. L. M. HOLMES, *Int. J. Magnetism* **6** (1974) 111.
4. L. M. HOLMES, L. G. VAN UITERT and G. W. HULL, *Solid State Commun.* **9** (1971) 1373.
5. L. M. HOLMES and L. G. VAN UITERT, *Phys. Rev. B* **5** (1972) 147.
6. H. SCHUCHERT, S. HUFNER and R. FAULHABER, *Z. Physik* **222** (1969) 105.

7. J. SIVARDIERE and S. QUEZEL-AMBRUNAZ, *C. R. Acad. Sci. Paris.* Ser **B273** (1971) 619.
8. H. KIMURA, T. NUMAZAWA, M. SATO, T. IKEYA and T. FUKUDA, *J. Appl. Phys.* **77** (1995) 432.
9. Y. OKANO, T. IKEYA, K. HOSHIKAWA and T. FUKUDA, *J. Cryst. Growth* **131** (1993) 616.
10. G. A. SLACK and D. W. OLIVER, *Phys. Rev. B* **4** (1971) 592.
11. T. NUMAZAWA, *J.A.P.* submitted.
12. P. V. E. MCCLINTOCK, I. P. MORTON, R. ORBACH and H. M. ROSENBERG, *Proc. Roy. Soc. Lond.* Ser **A298** (1967) 359.
13. J. CALLAWAY, *Phys. Rev.* **113** (1959) 1046

Received 10 April 1995
and accepted 8 July 1997